Relationship of Environmental Relative Humidity with North Atlantic Tropical Cyclone Intensity and Intensification Rate

Longtao Wu[1,2], Hui Su[1], Robert G. Fovell[3], Bin Wang[4], Janice T. Shen[1], Brian H. Kahn[1], Svetla M. Hristova-Veleva[1], Bjorn H. Lambrigtsen[1], Eric J. Fetzer[1], Jonathan H. Jiang[1]

[1]Jet Propulsion Laboratory
California Institute of Technology, Pasadena, California, USA
[2]Joint institute for Regional Earth System Science and Engineering
University of California, Los Angeles, Los Angeles, California, USA
[3]Department of Atmospheric and Oceanic Sciences
University of California, Los Angeles, Los Angeles, California, USA
[4]International Pacific Research Center
University of Hawaii at Manoa, Honolulu, Hawaii, USA

Highlights:

1. The first satellite data analysis to quantify the relationship of ERH with TC intensity and intensification rate.
2. ERH above the boundary layer generally decreases with time when TCs evolve. Near the surface, ERH stays approximately constant.
3. ERH is positively correlated with TC maximum intensity and more so with intensification rate. Substantial azimuthal asymmetry exists at radial distances greater than 400 km.
4. In the front-right quadrant relative to TC motion, rapid intensification is associated with a sharp decrease of ERH in the upper troposphere from the near to the far environment.

Abstract

Quantifying the relationship of large-scale environmental conditions such as relative humidity with hurricane intensity and intensity change is important for statistical hurricane intensity forecasts. Our composite analysis of 9 years of Atmospheric Infrared Sounder (AIRS) humidity data spanning 198 Atlantic tropical cyclones (TCs) shows that environmental relative humidity (ERH) above the boundary layer generally decreases with time as TCs evolve. Near the surface, ERH stays approximately constant. ERH is positively correlated with TC intensity and more so with intensification rate. Rapid intensifying TCs are associated with free tropospheric ERH more than 10% (relative to the averaged ERH for all TCs) larger than that for weakening TCs. Substantial azimuthal asymmetry in ERH is also found, especially for the TCs attaining the highest intensities and largest intensification rates at distances greater than 400 km away from the TC center. In the front-right quadrant relative to TC motion, rapid intensification is associated with a sharp gradient of ERH in the upper troposphere, with a decrease from the near

(40% between 400 hPa and 300 hPa) to the far environment (27%). The ERH gradient weakens with the decrease of intensification rate.

1. Introduction

While our understanding of tropical cyclones (TCs) has increased tremendously in the past several decades, TC genesis, spin-up and subsequent (especially sudden) intensity changes still present significant challenges. Official intensity forecasts from the National Hurricane Center (NHC) for Atlantic and Eastern North Pacific TCs have not shown much improvement in the last 20 years (DeMaria et al. 2007). This is because TCs are sensitive to many factors, within the storm and in its surrounding environment. For example, TCs are sensitive to vertical wind shear in the environment (DeMaria 1996; Frank and Ritchie 2001; Zehr 2003), which may be poorly forecasted by operational and research models. Also, relatively subtle variations in sea-surface temperature (SST) or ocean heat content can cause a TC intensity to shift several categories on the Saffir-Simpson scale within a short period of time (Sun et al. 2007).

The available moisture of the TC's environment represents another poorly understood influence on intensity, thereby presenting a limit to predictability. While high mid-tropospheric relative humidity (RH) appears to be necessary for rapid genesis and the attainment of maximum intensity (e.g., Kaplan and DeMaria 2003; Emanuel et al. 2004; Hendricks et al. 2010; Kaplan et al. 2010), dry air intrusions have a negative influence on TC evolution and intensification as dry air ingestion promotes the formation of cold downdrafts, which transport low θ_e air into the sub-cloud layer and storm inflow (e.g., Emanuel 1989). In an idealized modeling study, Braun et al. (2012) showed that low humidity air reaching the inner core induces asymmetric convective activity which weakens TCs (e.g., Nolan and Grasso 2003; Nolan et al. 2007). They further showed that the time for TCs to reach maturity varies with the proximity of dry air to the center

of circulation. When dry air is located 270 km away or further from the center of the vortex, its impact on TC intensity is insignificant.

Some studies (e.g., Barnes et al. 1983; Wang 2009) have shown that substantial and extensive moisture may also promote a net negative influence on TC strength by facilitating the formation of TC rainbands. The idealized modeling study of Hill and Lackmann (2009), which varied the environmental RH (ERH) in the region ≥ 100 km beyond the TC core, suggests that larger ERH results in the establishment of wider TCs with more prominent outer rainbands. However, TC development, as measured by time series of maximum 10 m wind speeds, was nearly insensitive to ERH despite the variation in rainband activity.

Kaplan and DeMaria (2003) examined the mid-tropospheric (850-700 hPa) ERH relation with rapidly intensifying (RI) TCs in the North Atlantic basin using the NHC HURDAT file (Jarvinen et al. 1984) and the Statistical Hurricane Intensity Prediction Scheme (SHIPS; DeMaria and Kaplan 1999) database. Hendricks et al. (2010) conducted composite analyses using the Navy Operational Global Atmospheric Prediction System (NOGAPS) global analysis. Both studies found that RI events over the Atlantic basin are associated with larger RH in the middle troposphere than non-RI events.

Analyses using satellite observations have been rather limited. Shu and Wu (2009) examined the influence of the Saharan air layer (SAL) on TC intensity with three years of RH data from the Atmospheric Infrared Sounder (AIRS) instrument. They defined the SAL intrusion in the AIRS RH data as the nearest location of dry (RH ≤ 30%) air between 600 and 700 hPa. Their analysis incorporating 37 TCs during 2005-2007 suggested that the dry SAL air had a favorable influence on TC intensity when present in the northwest quadrant of TCs but a

negative impact when the dry air approached to within 360 km, mostly in the southwest and southeast quadrants.

In this study, we examine all TCs over the North Atlantic from 2002 to 2010. The RH analyses are stratified with respect to the radial distance from the TC center, altitude, maximum intensity attained by the TCs, and intensification rate. The primary goals of this study are to quantify the relationships between ERH and TC intensity and intensification rate, and improve our understanding of the impact of environmental moisture on TC development. In particular, the results of this study may help improve statistical models, which still show the highest skill in TC intensity forecasts when compared to advanced mesoscale numerical models (Kaplan et al. 2010).

2. Data and Method

The Atmospheric Infrared Sounder (AIRS) onboard the Aqua satellite since 2002 has provided near-daily global coverage of the tropospheric water vapor profile from space (Divakarla et al. 2006; Susskind et al. 2003). The AIRS RH retrievals sample a broad ~1300 km swath at approximately 0130 and 1330 local time with a horizontal resolution of ~45 km near nadir. We use the Level 2 RH retrieval (version 5). The uncertainty of the RH retrieval is estimated to be 9% at 250 hPa and below (Gettelman et al. 2006). The six-hourly best track data for North Atlantic TCs are obtained from the Automated Tropical Cyclone Forecasting System (ATCF) at the NHC. This study summarizes the statistical behavior of 198 North Atlantic TCs, 74 of which achieved at least Category 1 intensity on the Saffir-Simpson scale, and were observed by AIRS during the period of 2002 and 2010.

Composites of ERH with respect to radial distance from the TC center, altitude, and quadrant with respect to TC motion are constructed. The TC center position at the local AIRS

observational time is linearly interpolated from the best track data. Three zones of radial distances from the TC center are defined: the *near environment* (200-400 km), *intermediate environment* (400-600 km) and *far environment* (600-800 km). Using the best track data, four quadrants are established relative to TC motion, numbered clockwise from the TC's front-right (Q1) to front-left sides (Q4). As TCs in the North Atlantic preferentially move westward, Q1 (Q4) roughly corresponds to the northwest (southwest) quadrant in geographic coordinate.

3. Results

3.1. Composite ERH as a function of time

Each TC is examined for the ±72 h period around its time of maximum intensity (T_{max}). A composite temporal evolution of ERH is obtained by averaging ERH for each TC at the same time relative to T_{max}. As shown in Fig. 1, the composite average ERH near surface (indicated by 1000-925 hPa layer) is about 82% for all four quadrants, with small variations throughout the 6-day period. ERH decreases with time at all altitudes above the boundary layer through the middle troposphere, and for all radial distances outward from the TC center. Furthermore, the magnitude of ERH declines from the near to the far environment. The average 500-600 hPa ERH in Q1 within the near environment is 56% at 72 h prior to peak intensity, dropping to 52% at T_{max} and further diminishing to 37% by T_{max}+72 h. Over that same 6-day period, the far environment ERH at the same level declines from 42% to 36%. This ERH trend is possibly a result of TC-induced subsidence bringing down dry air from above that desiccates the lower and middle troposphere. Land influences could also play a role as TCs translate west- and northwest-ward. The contributing physical factors to the drying effect with time warrants further investigation.

3.2. Composite ERH as a function of TC intensity

The maximum wind speed (V_{max}) from the best track data is used as an index for TC intensity and the ERH is then stratified with respect to TC intensity. Observed ERHs are normalized by the mean RH profile for the 198 TCs (see supplementary Fig. 1) and plotted as a function of V_{max} for different radial distances from the TC center in Fig. 2.

In the near environment, the TCs attaining the largest intensities (Category 5) possess a pronounced tendency towards having larger middle and upper tropospheric RH (Fig. 2a). This is seen in all quadrants and at all altitudes above the boundary layer. The composite ERH displays significant azimuthal asymmetry above the boundary layer at radial distances exceeding 400 km from the TC center (Figs. 2b and 2c). Relative to TC motion, the front quadrants (Q1 and Q4) have smaller mid-tropospheric RH while the rear quadrants (Q2 and Q3) are larger, especially in the far environment of Category 5 cases, where RH between 400 and 300 hPa (RH400) is 23% in Q1 and 51% in Q3.

3.3. Composite ERH as a function of TC intensification rate

The ERH is further stratified with respect to the TC intensification rate. The intensification rate at a particular time is defined as the V_{max} difference between that time and 6 hours later. Four intensity change bins are defined: *rapidly intensifying* (RI), *intensifying* (I), *neutral* (N), and *weakening* (W). RI corresponds to the top 5% and the other three equally sample intensification rates for the 198 TCs. The range of intensification rate for each category is given in Table 1.

ERH tends to be positively correlated with intensification rate, especially above the boundary layer in the near and intermediate environments (Fig. 3). RI is associated with larger than average ERH while weakening TCs have smaller than average ERH. The difference of free tropospheric ERH between RI and W is greater than 10% relative to the mean ERH for the 198

TCs. In Q1 within the intermediate environment, RH between 850 and 700 hPa (RH850) is 58% while weakening, increasing to 62% at the neutral stage, both being below average (Table 1). RH850 is about the average (64%) during the intensifying stage and further increases to above the average (66%) for RI. The RH at the RI stage is larger than that at the weakening and neutral stages with a statistical significance at the 95% confidence level. However, the difference of RH between the RI and intensifying stages is rather small and not always statistically significant, especially in the near environment (Table 1).

Azimuthal asymmetry above the boundary layer in the intermediate and far environments is evident, in particular during RI (Fig. 3). Similar to the composites with respect to intensity (Fig. 2), Q2 and Q3 are generally more moist, while Q1 and Q4 are drier. Note that in the front-right quadrant (Q1), RH400 in the near environment shifts from below (for W and N) to above average (for I and RI), representing a change in RH of about 9% (Table 1). However, for the far environment, the *lowest* ERH at this level is found at the RI stage for this quadrant, a decrease of 5% with respect to weakening TCs.

Thus, the horizontal moisture *gradient* between the near and far environments in Q1 is largest during the RI stage. This gradient is considerably smaller during the intensifying stage, and of opposite sign for weakening cases. The RI stage's combination of larger and smaller ERH in the near and far environments, respectively, may reflect the influence of the storm-induced circulation or is possibly a controlling factor for TC intensification. This unique feature has not been documented before. If substantiated, it could be a potential predictor for statistical hurricane forecast models.

4. Conclusion and Discussion

In this study, the ERH observed by AIRS is investigated in association with 198 TCs over the North Atlantic between 2002 and 2010. Composites of ERH with respect to radial distance from the TC center, altitude, and quadrant with respect to TC motion are constructed. The cases are also stratified with respect to time, TC intensity and intensification rate. The principal findings from this composite study of observational data are:

1. ERH in the free troposphere decreases with time as TCs evolve while ERH in the boundary layer stays approximately constant within ±72 hours from the time that TCs reach maximum intensity.
2. Higher intensity TCs tend to have larger ERH than lower intensity TCs.
3. TC intensification rate is generally positively correlated with ERH above the boundary layer. Rapidly intensifying TCs are associated with larger ERH than weakening and neutral TCs. However, the difference between rapidly intensifying and intensifying cases are not always statistically significant.
4. The azimuthal asymmetry of ERH becomes evident at radial distances > 400 km. The rear quadrants tend to have larger ERH and the front quadrants appear to have lower ERH.
5. In the front-right quadrant (Q1), a sharp decrease in upper tropospheric (above 400hPa) RH from the near to the far environment occurs during rapid intensification. This radial RH gradient is weaker for TCs with lower intensification rates. For weakening TCs, Q1 has slightly larger upper tropospheric ERH in the far environment than in the near environment.

The AIRS-centric investigation provides new insights regarding the environmental moisture within which TCs grow, decay, and propagate. The relationship of ERH with TC

intensity and intensification rate, especially its azimuthal and radial variations, may lead to improvements in TC intensity forecasts from statistical models.

There are remaining questions that warrant further investigation, particularly in regards to whether the observed relationships represent the impact of ERH on TC development, or a more complex set of nonlinear interactions between a TC and its environment. For example, is the dry air in the front-right quadrant in the intermediate and far environments providing favorable (by suppressing rainband convection) or detrimental influence on TC intensification? Or, is it simply a result of the TC circulation (from subsidence drying)? Additional numerical model experiments could help clarify the role of environmental moisture in TC evolution. This observational analysis will be valuable to validation of numerical and statistical models, and can provide guidance for alterations to the physical parameterizations in numerical models.

Acknowledgements

The authors thank Dr. Sundararaman Gopalakrishnan and Dr. Tomislava Vukicevic for valuable discussions, and Dr. Mark DeMaria for suggestions. The work is conducted at the Jet Propulsion Laboratory, California Institute of Technology, under contract with NASA. The authors thank the funding support from the NASA HSRP program.

References

Barnes, G. M., E. J. Zipser, D. Jorgensen, and F. Marks Jr., 1983: Mesoscale and convective structure of a hurricane rainband. *J. Atmos. Sci.*, 40, 2127–2137.

Braun, S. A., J. A. Sippel, D. S. Nolan, 2012: The Impact of Dry Midlevel Air on Hurricane Intensity in Idealized Simulations with No Mean Flow. *J. Atmos. Sci.,* 69, 236–257. doi: http://dx.doi.org/10.1175/JAS-D-10-05007.1

DeMaria, M., 1996: The Effect of Vertical Shear on Tropical Cyclone Intensity Change. *J. Atmos. Sci.*, 53, 2076–2088. doi: http://dx.doi.org/10.1175/1520-0469(1996)053<2076:TEOVSO>2.0.CO;2

DeMaria, M., J. Kaplan, 1999: An Updated Statistical Hurricane Intensity Prediction Scheme (SHIPS) for the Atlantic and Eastern North Pacific Basins. Wea. Forecasting, 14, 326–337. doi: http://dx.doi.org/10.1175/1520-0434(1999)014<0326:AUSHIP>2.0.CO;2

DeMaria, M., J. A. Knaff, and C. Sampson, 2007: Evaluation of long-term trends in tropical cyclone intensity forecasts. *Meteor. Atmos. Phys.*, 97, 19–28.

Divakarla, M. G., C. D. Barnet, M. D. Goldberg, L. M. McMillin, E. Maddy, W. Wolf, L. Zhou, and X. Liu (2006), Validation of Atmospheric Infrared Sounder temperature and water vapor retrievals with matched radiosonde measurements and forecasts, *J. Geophys. Res.*, 111, D09S15, doi:10.1029/2005JD006116.

Emanuel, K.A., 1989: Dynamical theories of tropical convection. *Aust. Meteor. Mag.*, 37, 3-10.

Emanuel, K., C. DesAutels, C. Holloway, R. Korty, 2004: Environmental control of tropical cyclone intensity. *J. Atmos. Sci.*, 61, 843–858. doi: http://dx.doi.org/10.1175/1520-0469(2004)061<0843:ECOTCI>2.0.CO;2

Frank, W. M., E. A. Ritchie, 2001: Effects of Vertical Wind Shear on the Intensity and Structure of Numerically Simulated Hurricanes. *Mon. Wea. Rev.*, 129, 2249–2269. doi: http://dx.doi.org/10.1175/1520-0493(2001)129<2249:EOVWSO>2.0.CO;2

Gettelman, Andrew, Eric J. Fetzer, Annmarie Eldering, Fredrick W. Irion, 2006: The Global Distribution of Supersaturation in the Upper Troposphere from the Atmospheric Infrared Sounder. *J. Climate*, **19**, 6089–6103. doi: http://dx.doi.org/10.1175/JCLI3955.1

Hendricks, E. A., M. S. Peng, B. Fu, T. Li, 2010: Quantifying Environmental Control on Tropical Cyclone Intensity Change. *Mon. Wea. Rev.*, 138, 3243–3271. doi: http://dx.doi.org/10.1175/2010MWR3185.1

Hill, K. A., G. M. Lackmann, 2009: Influence of Environmental Humidity on Tropical Cyclone Size. *Mon. Wea. Rev.*, 137, 3294–3315. doi: http://dx.doi.org/10.1175/2009MWR2679.1

Jarvinen, B. R., C. J. Neumann, and M. A. S. Davis, 1984: A tropical cyclone data tape for the North Atlantic basin, 1886–1983: Contents, limitations, and uses. NOAA Tech. Memo. NWS NHC 22, Miami, FL, 21 pp. [Available from National Technical Information Service, 5285 Port Royal Rod., Springfield, VA 22151.]

Kaplan, J., and M. DeMaria, 2003: Large-scale characteristics of rapidly intensifying tropical cyclones in the North Atlantic basin, *Wea. Forecasting*, 18:6,1093-1108.

Kaplan, J., M. DeMaria, J. A. Knaff, 2010: A Revised Tropical Cyclone Rapid Intensification Index for the Atlantic and Eastern North Pacific Basins. *Wea. Forecasting*, 25, 220–241. doi: http://dx.doi.org/10.1175/2009WAF2222280.1

Nolan, D. S., L. D. Grasso, 2003: Nonhydrostatic, Three-Dimensional Perturbations to Balanced, Hurricane-Like Vortices. Part II: Symmetric Response and Nonlinear Simulations. *J. Atmos. Sci.*, 60, 2717–2745. doi: http://dx.doi.org/10.1175/1520-0469(2003)060<2717:NTPTBH>2.0.CO;2

Nolan, D. S., Y. Moon, D. P. Stern, 2007: Tropical Cyclone Intensification from Asymmetric Convection: Energetics and Efficiency. *J. Atmos. Sci.*, 64, 3377–3405. doi: http://dx.doi.org/10.1175/JAS3988.1

Shu, S., and L. Wu (2009), Analysis of the influence of Saharan air layer on tropical cyclone intensity using AIRS/Aqua data, *Geophys. Res. Lett.*, 36, L09809, doi:10.1029/2009GL037634.

Sun, D. L., Kafatos, M., Cervone, G., Boybeyi, Z., Yang, R. X. (2007). Satellite microwave detected SST anomalies and hurricane intensification. *NATURAL HAZARDS*, 43(2), 273-284.

Susskind, J., C. D. Barnet, and J. Blaisdell (2003), Retrieval of atmospheric and surface parameters from AIRS/AMSU/HSB data under cloudy conditions, *IEEE Trans. Geosci. Remote Sens.*, *41*(2), 390–409.

Wang, Y., 2009: How Do Outer Spiral Rainbands Affect Tropical Cyclone Structure and Intensity? *J. Atmos. Sci.*, 66, 1250–1273. doi: http://dx.doi.org/10.1175/2008JAS2737.1

Zehr, R. M., 2003: Environmental Vertical Wind Shear with Hurricane Bertha (1996). *Wea. Forecasting*, 18, 345–356. doi: http://dx.doi.org/10.1175/1520434(2003)018<0345:EVWSWH>2.0.CO;2

List of Figures

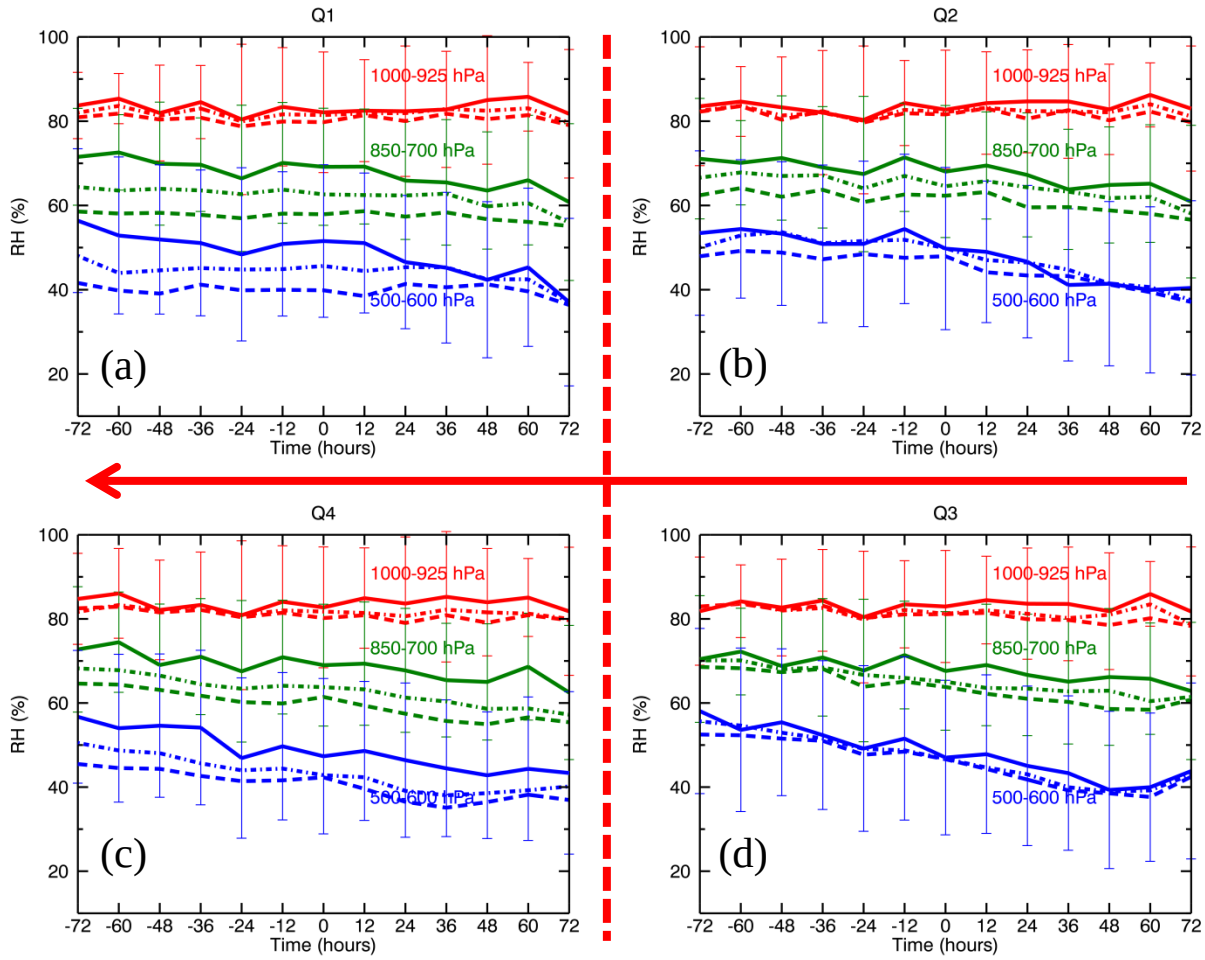

Figure 1. Time evolution of tropospheric RH at three pressure layers (1000-925 hPa in red; 850-700 hPa in green; 600-500 hPa in blue) averaged at three radial distances (near environment in solid line; intermediate environment in dash dot line; and far environment in dashed line), composited for 198 tropical cyclones over the North Atlantic Ocean from 2002 to 2010. Standard deviation is shown for near environment. The time "0" corresponds to the time of maximum TC intensity. (a) quadrant 1 (Q1); (b) quadrant 2 (Q2); (c) quadrant 4 (Q4); (d) quadrant 3 (Q3). The red arrows indicate the preferential translation direction of TCs in the North Atlantic.

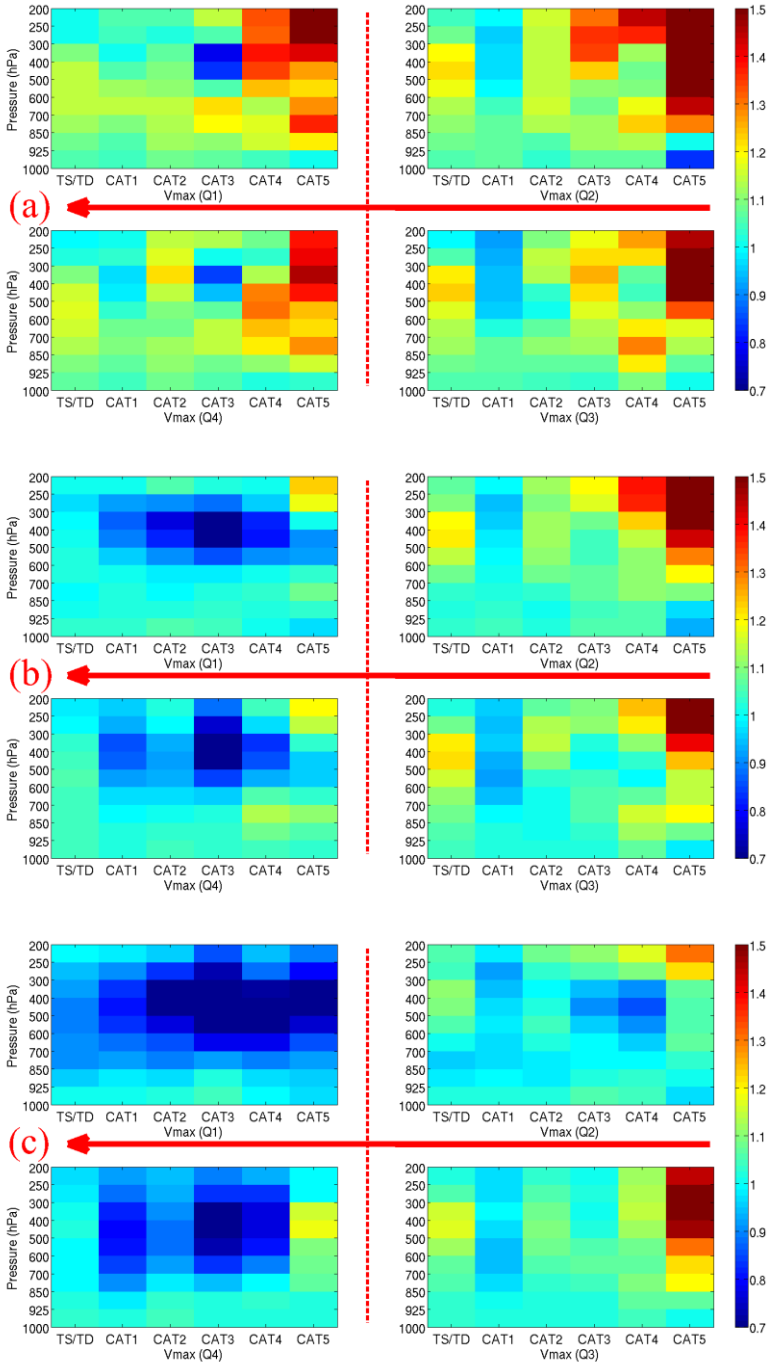

Figure 2. Normalized RH as a function of maximum TC intensity at three radial distances: (a) near environment; (b) intermediate environment; and (c) far environment. The normalization is with respect to the mean RH profile averaged for all 198 TC cases over the North Atlantic from 2002 to 2010 (see supplementary Figure 1). The four panels in each figure represent the four quadrants numbered from the front-right side of the TC (Q1) clockwise around to the front-left quadrant (Q4). The red arrows indicate the preferential translation direction of TCs in the North Atlantic.

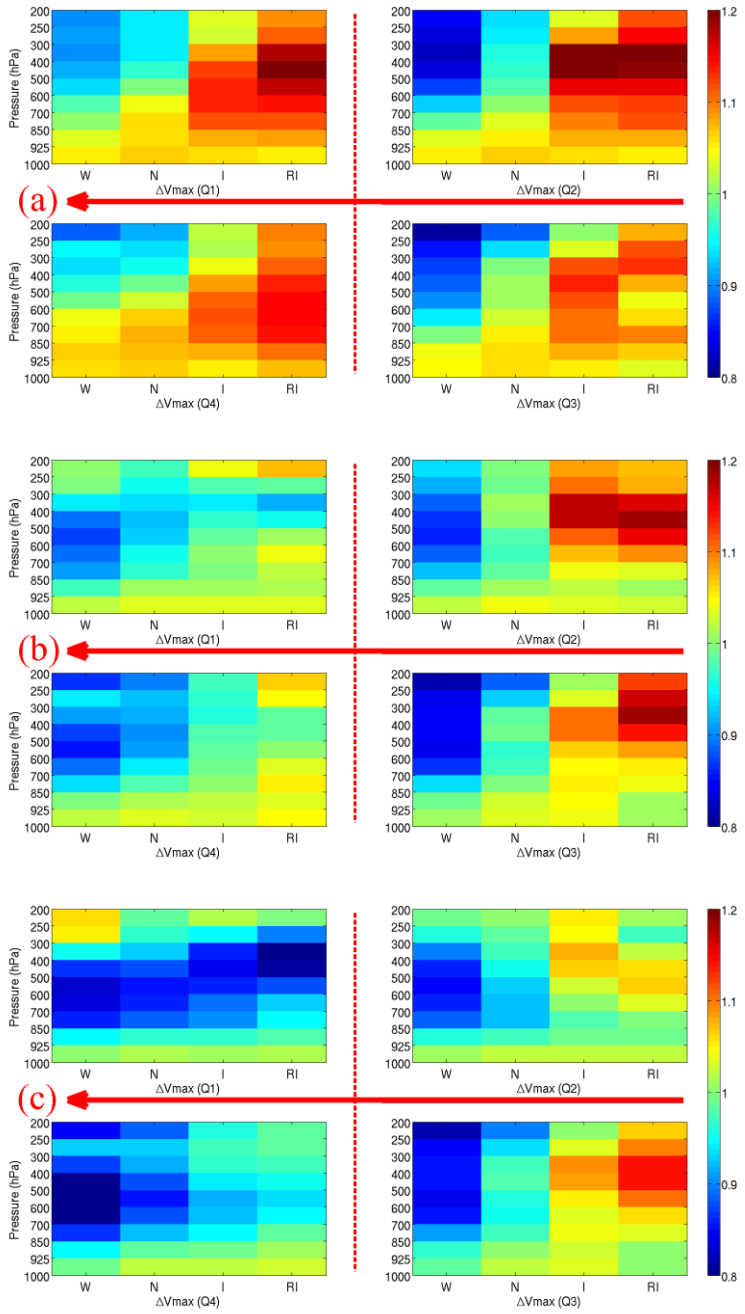

Figure 3. Normalized RH as a function of TC intensification rate at three radial distances: (a) near environment; (b) intermediate environment; and (c) far environment. The normalization is with respect to the mean RH profile averaged for all 198 TC cases over the North Atlantic from 2002 to 2010 (see supplementary Figure 1). The four panels represent the four quadrants numbered from the front-right side of the TC (Q1) clockwise around to the front-left quadrant (Q4). W: weakening (ΔV_{max}< -1.25 m s^{-1} per 6 hrs); N: neutral (-1.25 < ΔV_{max}< 1.75 m s^{-1} per 6 hrs); I: Intensifying (1.75 < ΔV_{max}< 4.75 m s^{-1} per 6 hrs); RI: rapidly intensifying (ΔV_{max}> 4.75 m s^{-1} per 6 hrs). The red arrows indicate the preferential translation direction of TCs in the North Atlantic.

List of tables

Table 1. Averaged RH for weakening (W: $\Delta V_{max} < -1.25$ m s^{-1} per 6 hrs), neutral (N: $-1.25 \leq \Delta V_{max} < 1.75$ m s^{-1} per 6 hrs), Intensifying (I: $1.75 \leq \Delta V_{max} < 4.75$ m s^{-1} per 6 hrs), rapidly intensifying (RI: $\Delta V_{max} > 4.75$ m s^{-1} per 6 hrs) cases, and the differences between RI and the other groups. Intensification rate (ΔV_{max}) is defined as the 6-hour V_{max} change. The second column is the mean value averaged for all 198 TC cases. The bold face denotes statistical significance at the 95% confidence level. The unique feature of RH400 in Q1 is highlighted in red.

Quantity	Mean	Quadrant	Distance	W	N	I	RI	RI – W	RI – N	RI – I
RH850 (850-700 hPa RH, %)	64.34	Q1	Near	64.55	68.18	71.84	71.90	**7.35**	**3.72**	0.06
			Intermediate	58.35	62.31	64.18	65.89	**7.54**	**3.58**	**1.71**
			Far	55.48	56.91	58.22	60.87	**5.39**	**3.96**	**2.65**
		Q3	Near	64.15	67.88	71.00	70.63	**6.48**	**2.75**	-0.07
			Intermediate	59.94	64.26	67.81	66.90	**6.96**	**2.64**	-0.91
			Far	58.33	62.60	66.82	66.36	**8.03**	**3.74**	-0.47
RH400 (400-300 hPa RH, %)	34.06	Q1	Near	30.82	32.12	36.91	40.16	**9.34**	**8.04**	**3.25**
			Intermediate	31.94	31.77	32.04	31.25	-0.69	-0.52	-0.79
			Far	32.43	31.50	29.26	27.45	**-4.98**	**-4.05**	**-1.71**
		Q3	Near	29.73	33.88	37.90	38.41	**8.68**	**4.53**	0.51
			Intermediate	28.75	33.58	37.57	40.35	**11.60**	**6.77**	**2.78**
			Far	28.96	33.11	37.19	38.87	**9.91**	**5.76**	**1.69**

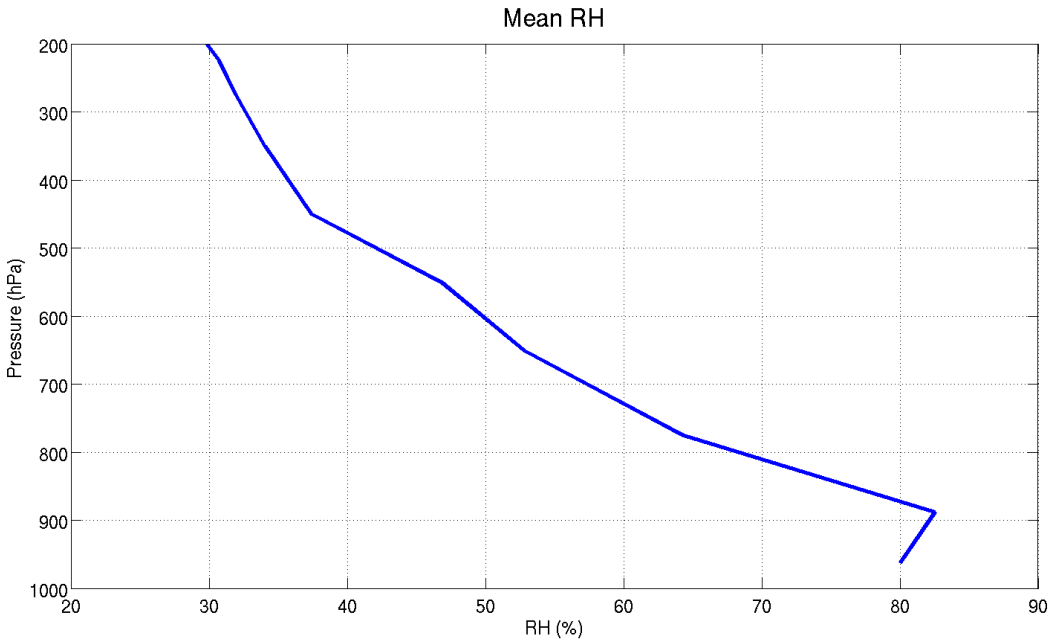

Supplementary Figure 1: The mean RH profile averaged for all 198 TC cases over the North Atlantic from 2002 to 2010.